Supplemental Information for Manuscript: Dual Colorimetric and Electrochemical Detection of Food and Waterbonre Bacteria from A Single Assay

Jaclyn A. Adkins,[a] Katherine Boehle,[b] Colin Friend,[c] Briana Chamberlain,[d] Bledar Bisha,[e] Charles S. Henry[a]*

Department of [a]Chemistry, [b]Chemical Biology, [c]Biomedical Engineering, and [d]Chemical and Biological Engineering, Colorado State University, Fort Collins, Colorado 80523, United States

[e]Department of Animal Science, University of Wyoming, Laramie, Wyoming, 82071, United States

*E-mail: Chuck.Henry@colostate.edu. Phone: +1-970-491-2852.

Table of Contents

Section S1. Materials and Reagents. Potassium chloride (KCl), potassium ferricyanide ($K_3Fe(CN)_6$), and Whatman #1 filter paper were purchased from Fisher Scientific (Fairlawn, NJ). Potassium ferrocyanide ($K_4Fe(CN)_6$) was purchased from Mallinckrodt Chemical Works (St. Louis, MO). Carbon ink and Graphite (<20-μm diameter) were purchased from Ercon (Warham, MA) and Sigma (St. Louis, MO) respectively. High-purity silver ink was purchased from SPI Supplies (West Chester, PA). *p*-Aminophenol (PAP) was purchased from EMD Millipore (VWR, Billerica, MA). Sodium chloride (KCl), potassium phosphate monobasic (KH_2PO_4), potassium phosphate dibasic (K_2HPO_4), β-galactosidase (β-gal), β-glucosidase, β-glucuronidase (β-glucr), *p*-nitrophenyl-β-D-glucopyranoside (PNP-Gluco), and *p*-nitrophenyl-β-D-glucuronide (PNP-glucr) were purchased from Sigma. *p*-Nitrophenol (PNP) and *p*-nitrophenyl-β-D-galactopyranoside (PNP-gal) were purchased from TCI America (VWR, Portland, OR). *o*-Nitrophenol (ONP) and *o*-nitrophenyl-β-D-galactopyranoside (ONP-gal) were purchased from ACROS Organics™ (Thermo Fisher Scientific, Waltham, MA). *p*-Aminophenyl-β-D-galactopyranoside (PAP-gal) was purchased from Biosynth (Itasca, IL). *o*-Nitrophenyl-β-D-glucopyranoside (ONP-Gluco) was purchased from Alfa Aesar (VWR, Haverhill, MA). Enzyme, substrate, and stock solution aliquots were stored at -20°C prior to use. Fresh aliquots were thawed prior to use daily. All reagents were used as received without further purification. All electrochemical measurements were done using an eDAQ EA161 Potentiostat and EC201 e-Corder (Denistone East, Australia). Copier transparency sheets PP2200 and 2-in-wide Scotch® brand heavy duty clear shipping packaging tape were purchased from 3M (St. Paul, MN). Boise®Aspen® 30 multi-use recycled copy paper was purchased from OfficeMax®. Paper devices were printed using a Xerox (Norwalk, CT) ColorCube 8870 wax printer and stencils, paper and tape components were cut using a 30 W Epilog (Golden, CO) Zing Laser Cutter and Engraver. Wax designs were melted using a Fisher Scientific IsoTemp hotplate. Spectrophotometric detection was performed using Biotek Synergy 2 (BioTek Instruments, Inc., Winooski, VT) plate reader. A Stomacher 400 Lab-Blender by Tekmar was used to mix/wash food samples in media and cells were lysed using a Misonix XL-2000 Series (Qsonica, LLC., Newtown, CT) probe sonicator.

Section S2. Device Fabrication. Briefly, CorelDRAW software was used to design geometries for wax barriers and laser-cut stencils. A wax printer was used to print wax designs onto the copy paper surface that was then melted through the paper using a hotplate at (150°C) for 60 s to form hydrophobic wax barriers (Figure 1A). Packing tape was used to seal the back of the printed circles to form wells. Paper-based well plates consisted of 7 columns and 12 rows for a total of 84 wells that were each 6-mm in diameter (inner) after melting and held 50 μL of total solution volume.

Electrodes were printed onto transparency film, Whatman, or copy paper sheets by squeegeeing a carbon ink mixture (1:2 ratio by mass of graphite to carbon ink) through a laser-cut transparency film stencil to form electrode geometries (Figure S1 and Figure 2). The commercial ink was intended for screen-printing purposes; however, stencil-printing is a simpler method for mask preparation. Therefore, to make the ink consistency amenable for stencil-printing manipulation, the addition of graphite powder was used to create a more conductive and viscous ink and minimize leaking beneath the stencil. Similar to paper-based devices, the entire printed sheet is flexible and contains 240 devices (Figure 1A and B) with electrode geometries shown in Figure 1C. After drying for 60 min at 65°C, a small layer of silver paint was applied to

the reference electrode within the well to serve as a Ag/AgCl reference with the presence of 0.4 M chloride in tested solutions (Figure 1C). Each electrode well holds 30 μL of total solution volume (Figure 1D).

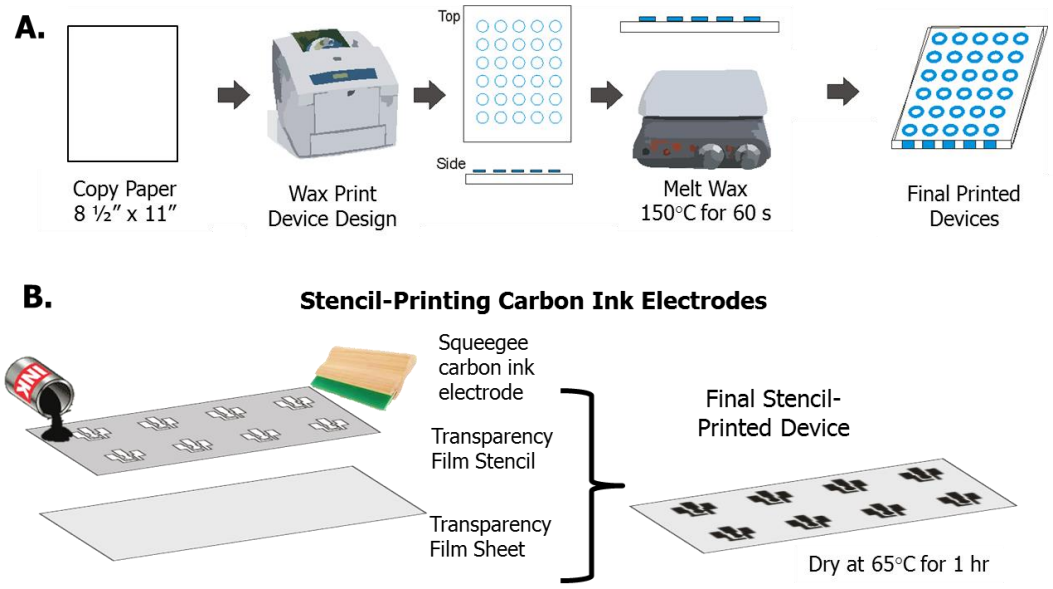

Figure S1. Fabrication schemes for fabrication of (A) wax printed paper-based well devices and (B) stencil-printed transparency film-based carbon electrodes.

Section S3. Colorimetric Detection. A white paper lining was used in the box to reflect and distribute light from the camera flash more evenly, and decrease the appearance of low lighting regions. Blank spot rows were further used to normalize lighting conditions. Figure S2 shows the process of image analysis using NIH ImageJ software. First, the image was split into RGB color channels and the blue color channel was selected for optimal analysis of the yellow formed products. The channel was then inverted, so that as color intensity due to product formation increased so did the measured mean grey intensity. The mean intensity of each spot test was measured, and normalized to a background lighting condition by subtracting the average mean intensity of the water spots on each side of the sample as shown in Figure S2.

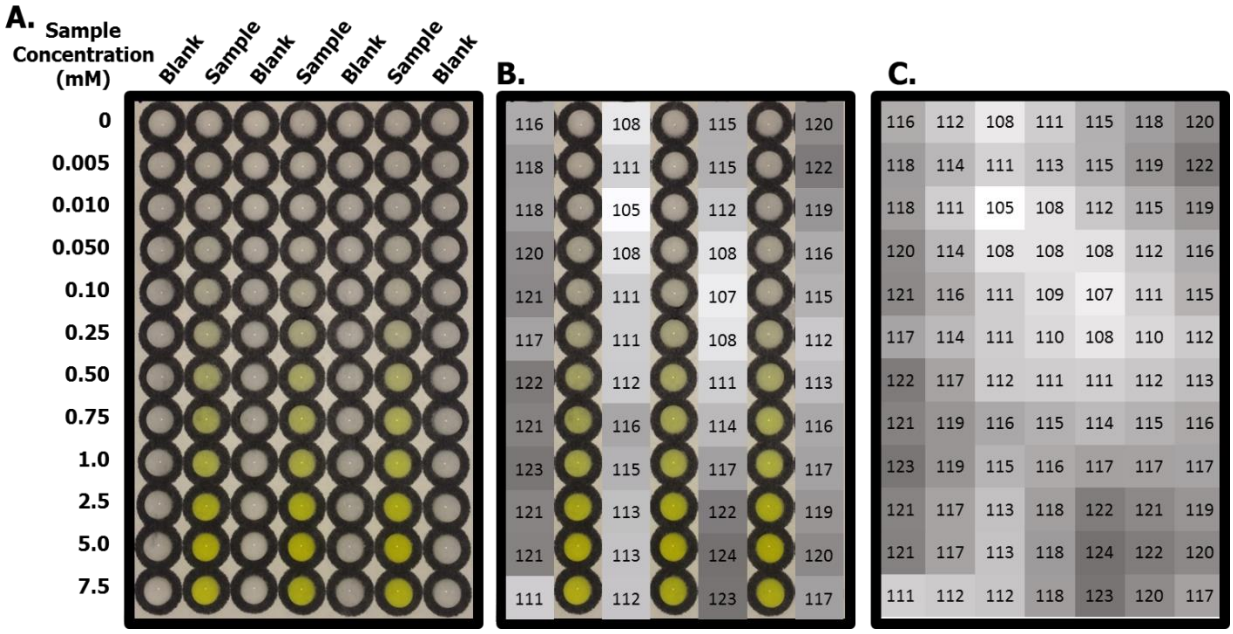

Figure S2. Background normalization process for (A) an example PNP calibration image, where (B) the blank spots are converted to an intensity unit and are shown shaded dark to light from highest to lowest intensity respectively. (C) The spots surrounding a sample spot are averaged to form an average background lighting condition for that sample to be subtracted from the measured sample intensity.

Section S4. Buffer Preparation. Buffer and pH optimization were performed using phosphate-buffered saline (PBS), phosphate-citrate buffered saline (PCS buffer), and carbonate buffered saline. PBS buffers of different pH were made by mixing KH_2PO_4 and Na_2HPO_4 to form 0. 2 M phosphate at pH 5.6, 6, 6.5, 7, 7.5, and 8 in 0.4 M KCl in weight ratios (g:g) as follows: pH 5.6 (22.4:3.49), pH 6 (21.05:6.60), pH 6.5 (16.44:16.90), pH 7 (9.36:32.73), pH 7.5 (3.84:45.07), pH 8 (1.27:50.81) per L in 0.4 M KCl. Different pH PCS buffers were made by mixing stock solutions of 0.2 M Na_2HPO_4 and 0.1M citric acid monohydrate both with 0.4 M KCl into volume ratios (mL:mL) as follows: pH 3 (20.55:79.45), pH 4 (38.55:61.45), pH 5 (48.50:51.50), pH 6 (63.45:36.85), pH 7.5 (93.25:6.75). Carbonate buffers were made using 0.1 M Na_2CO_3 and 0.1 M $NaHCO_3$ in ratios (mL:mL) as follows: pH 9.5 (30:70), pH 10 (55:45), and pH 10.5 (80:20). Final pH values for each buffer were read using a pH meter.

Section S5. Electrochemical Platform Optimization. While it is unclear why the copy paper's performance was lowest, a few hypotheses have been proposed. The smaller thickness and lower porosity of the paper beneath the electrode when compared to the filter paper-based electrode would lead to less solution interaction with the electrode surface than the higher pore size filter paper-based electrode. Alternatively, the fibers in copy paper could expand more than in filter paper or there could be an issue with the fillers used in copy paper causing increased peak splitting and decreased peak current. Further investigations into this finding were not pursued at this point in the project.

For comparison purposes, electrodes made on transparency film sheets of poly(ethylene terephthalate) (PET) were also studied. When using the transparency film sheets, the wax

printing step was omitted from the fabrication process. Using wax in the paper devices resulted in a thin layer of wax that spread throughout the depth of the paper and surrounded the cellulose fiber surfaces. However, when the same amount of wax was printed onto the non-porous transparency film surface, a thicker layer formed. When the electrode was printed over the top of the wax, the solvents used to disperse the carbon ink materials also partially dissolved the wax barriers beneath the electrode. Once the ink dried, the nonconductive wax was incorporated into the electrode, increasing electrode resistance and giving poor electrochemical behavior. Because the transparency film is nonporous and the carbon ink is slightly hydrophobic, the electrode geometry itself created a barrier that was maintained by solution surface tension without the need for a wax barrier

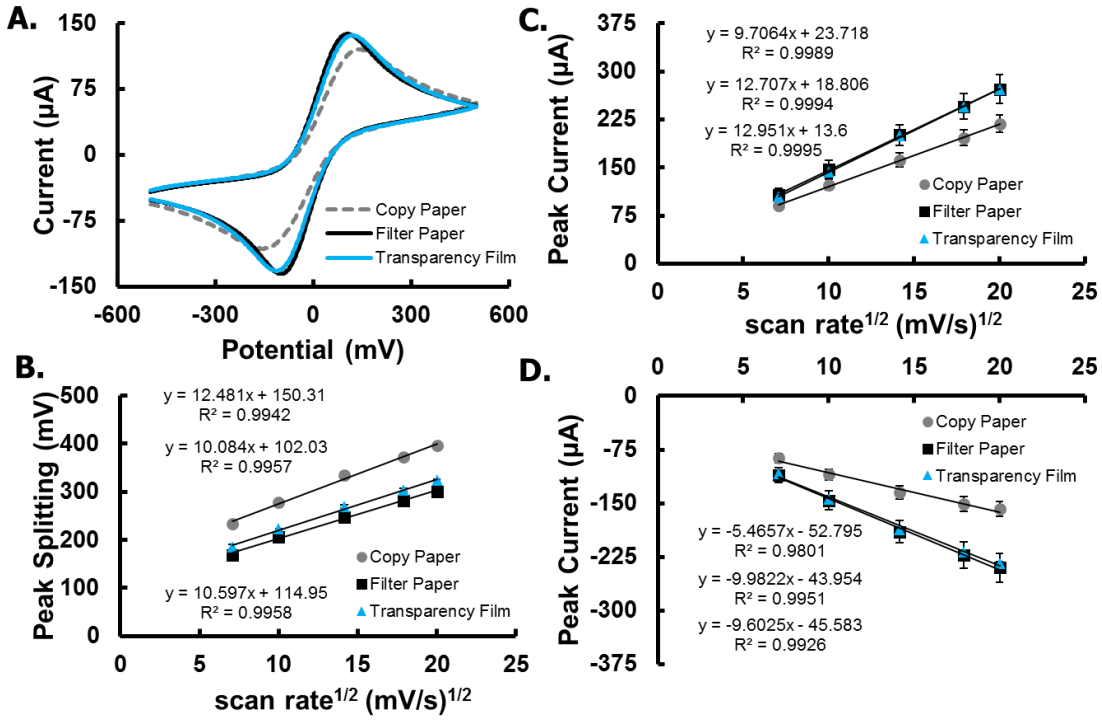

Figure S3. Electrochemical characterization of copy paper-, Whatman 1 filter paper-, and Transparency film-based electrodes using cyclic voltammetry. (A) Representative CVs using each material at 100 mV/s of for 5 mM $K_3Fe(CN)_6/K_2Fe(CN)_6$ in 0.5 M KCl and B) resulting peak splitting, (C) oxidative peak current, and (D) reductive peak current plotted with the square root of the applied scan rate. (n=3)

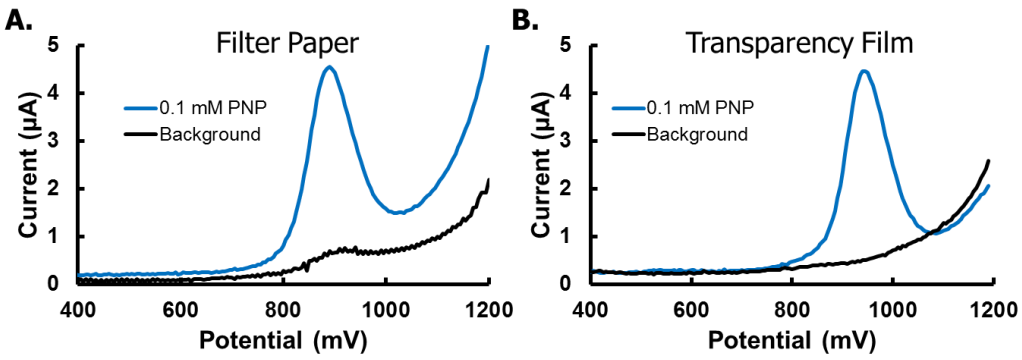

Figure S4. Detection of background PBS electrolyte and 0.1 mM PNP at (A) Whatman 1 filter paper-based SPCEs and (B) transparency film-based SPCEs. (RE=Ag/AgCl)

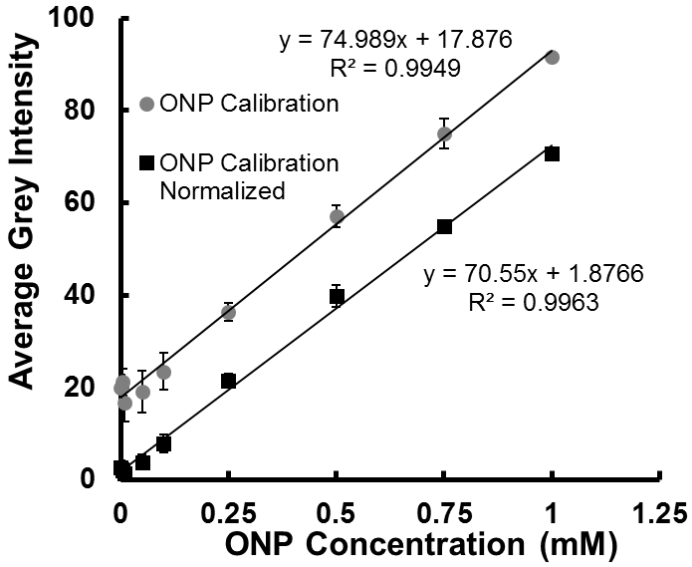

Figure S5. Measured average grey intensity for ONP calibration in paper-based wells with and without background lighting normalization. (n=3)

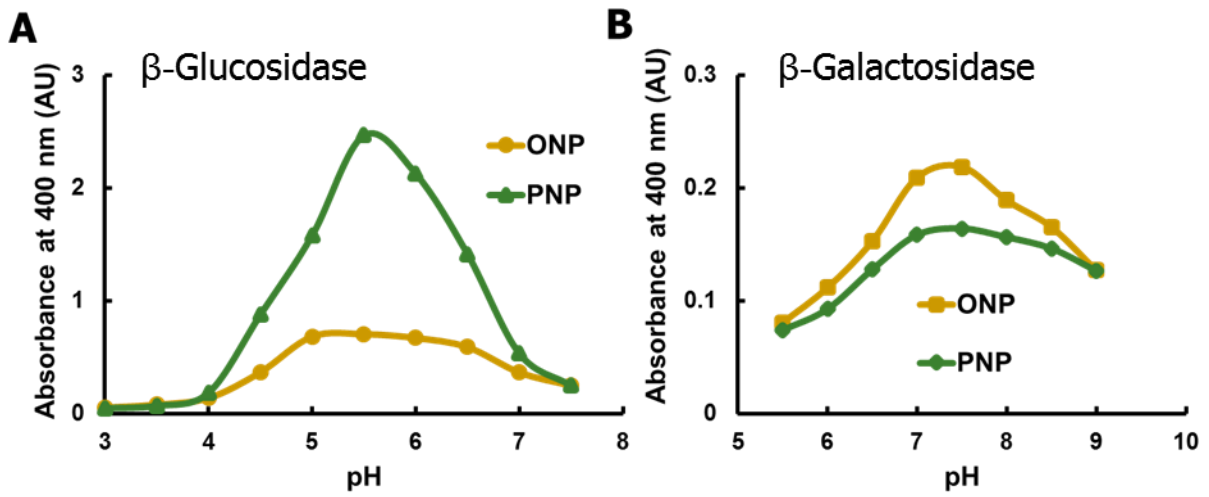

Figure S6. Optimal pH measurements for A) ONP-gluco and PNP-gluco reacted with β-gluco in PCS buffer, and ONP-gal and PNP-gal reacted with β-gal in PBS buffer. (n=3)

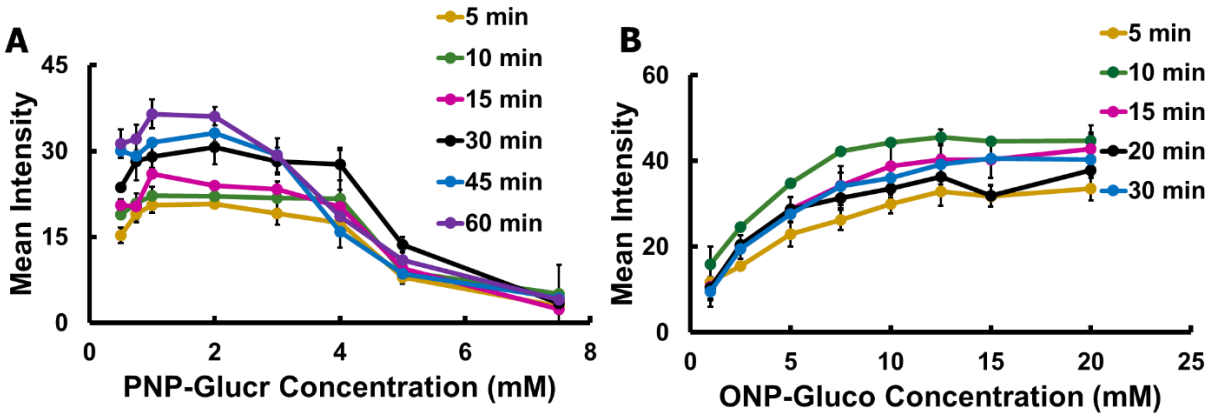

Figure S7. Measured average grey intensity results of enzymatically formed product A) PNP and B) ONP from varying concentrations of substrate PNP-Glucr and ONP-Gluco respectively. Enzymes for ONP-Gluco and PNP-Glucr are β-gluco and β-glucr respectively. (n=3)

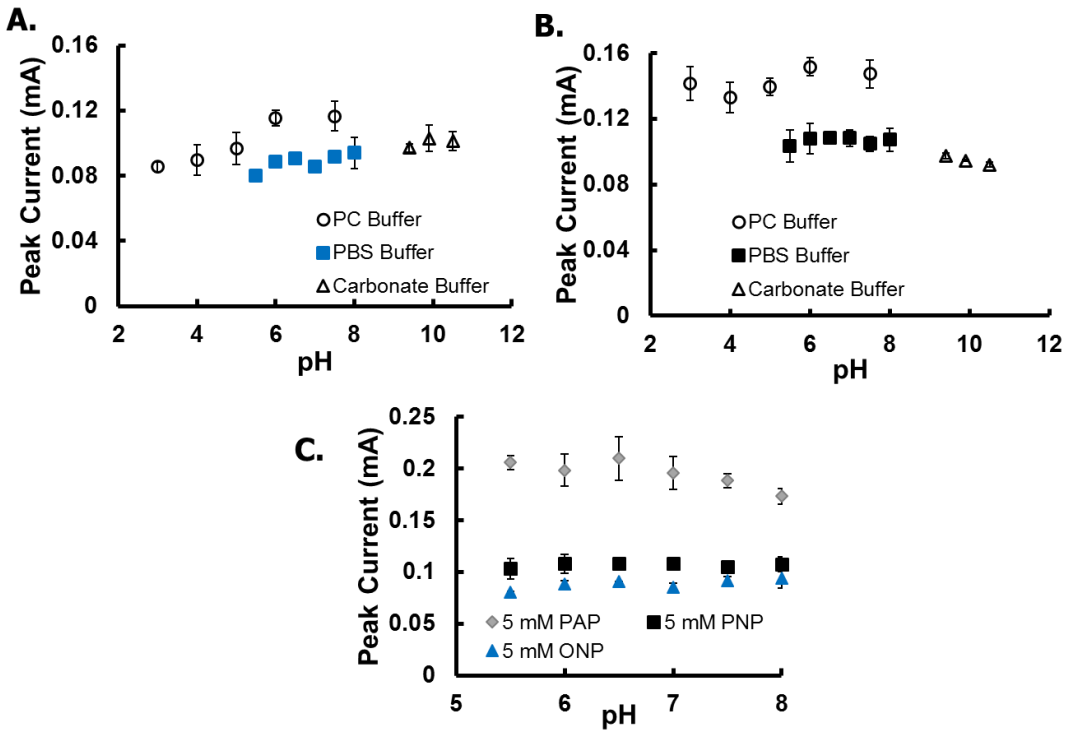

Figure S8. Buffer and pH SWV study for optimal detection of 5 mM (A) PNP and (B) ONP in PBS, PC, and carbonate buffers, and (C) resulting overlay of PNP, ONP, and PAP in PBS buffer (n=3)

PAPG Electrochemical Detection

		Time (hr)			
	C/I	4	8	12	24
E. coli P14	10^1	-	56.64	110.23	37.19
	10^2	-	43.97	108.47	78.84
	10^3	-	66.15	117.77	75.12
E. coli O157:H7	10^1	-	40.60	nd	95.82
	10^2	-	110.03	nd	106.98
	10^3	-	112.48	nd	111.65
Sprout	C	8.96	56.92	nd	27.48
	I	15.04	47.61	nd	32.63
Water	C	-	-	nd	-
	I	-	90.53	nd	32.62

Figure S9. Heat map showing average (n=3) of electrochemical peak current (µA) detection of PAP produced from PAP-gal enzymatic assays measured after 1 h of assay reaction. Two pure culture *E. coli* strains were diluted to low concentrations (CFU/mL) and sprout and water samples either inoculated (I) or control (C) were measured with pre-enrichment culture time. (-) Indicates signals below the detection limit, (nd) fnot determined.